

Impact of Thermal Radiation and Viscous Dissipation on Heat and Mass Transfer in *MHD* Non-Darcian flow of Micropolar Fluid along an Inclined Porous Plate embedded in Porous Media

Hina Yadav¹, Mamta Goyal²

¹Department of Mathematics, University of Rajasthan, Jaipur-302004, India ²Department of Mathematics, University of Rajasthan, Jaipur-302004, India

Abstract: The process of heat and mass transfer in *MHD* time independent two-dimensional flow of micropolar fluid along an inclined porous plate embedded in a non-Darcian porous media with thermal radiation and viscous dissipation is analyzed. Momentum boundary layer equation consider transverse magnetic field in this study. Momentum equation is effected by Non-Darcian flow model which taken to characterized the porous media. Similarity transformation technique is utilized to acquire non linear coupled ordinary differential equations from governing partial differential equations. Numerical solution of reduced equations is obtained by the Runge-Kutta scheme associated with shooting technique. Impact of various non-dimensional parameters on velocity, microrotation, temperature and concentration profile are discussed through graphical representations.

2020 Mathematics Subject Classification: 76W05, 76D05, 76Sxx, 80A19, 78A40.

Key words: *MHD*, Micropolar fluid, Non-Darcy flow, Porous medium, Heat and mass transfer, Radiation, Viscous dissipation.

1 Introduction

Use of non-Newtonian fluids in the engineering and industrial processes has boosted researchers and engineers interest to examine the attributes and behavior of these fluids under different flow models. Such type of fluids are especially useful in real industrial applications in several fields like in polymer engineering, crude oil extraction, food processing, natural science, geophysics, petroleum industries and chemical industries, etc. Various models regarding non-Newtonian fluids have been communicated considering different physical properties for example Casson fluid, Jeffery fluid, Williamson fluid, Maxwell fluid, Nano fluid with non-Newtonian base fluid, Johnson-Segalman fluid, Power law fluid and Micropolar fluid etc. [1]. The basic theory of micropolar fluids has been derived by Eringen [2]. This approach is to be effective to analyzing the behavior of non-Newtonian fluids. Eringen [3] has been developed the theory of thermomicropolar fluids. Micropolar fluids have interior micro shape in which coupling among the spin of every particle, this microrotational velocity is also accounted. These structures are come into view in polymer technology. They consists of rigid, irregular orientation or spherical particle along own spin and micro rotation, dump in viscous medium.

Currently Heat and mass transfer through porous media is center of intensive research because of its important practical applications for example freshwater supplies for different localities, drying, moisture migration in fibrous insulation, nuclear and petroleum waste disposal, to control the pollutant spread in ground water, chemical reactors, heat exchangers electronic cooling, food industries etc. Sharma and Sinha [4] analyzed impact of velocity slip and thermal slip in presence of non-uniform magnetic field on *MHD* mixed convective flow along vertical porous plate. Dulal pal and Sewli chatterjee have

analyze heat and mass transfer characteristic considering non-darcian model for micropolar fluid over a stretching sheet placed in porous medium in presence of non-uniform heat source, thermal radiation with uniform magnetic field [5]. Muhammad et al. have done theoretical analysis of Chemically reactive flow of micropolar fluid in presence of viscous dissipation and Joule heating using series solution [6]. Tripathy et al. investigate the non-Darcian flow model of *MHD* micropolar fluid along stretching sheet placed in porous medium [7]. Radiation and chemical reaction significance on Heat and mass transfer in *MHD* natural convection of micropolar fluid considering a truncated cone studied by Chamkha et al. [8]. It is now proposed to study impact of thermal Radiation and viscous dissipation on heat and mass transfer in *MHD* non-darcian flow of micropolar fluid along an inclined porous plate embedded in porous media.

2 Mathematical Formulation

In the present analysis, Mixed convective two dimensional time independent non-Darcy flow of viscous incompressible Micropolar fluid along an inclined porous plate through porous medium is considered. Here x -axis taken in direction of porous Plate. y -axis measured perpendicular to it. Let u and v are velocity components along x and y axis respectively. Magnetic field is

enforced transversely to porous plate in presence of radiation and viscous dissipation phenomena. Considering above postulation the governing equations of continuity, linear momentum, angular momentum, energy and mass transfer of present flow are given below:

$$\frac{\partial u}{\partial x} + \frac{\partial v}{\partial y} = 0, \quad (2.1)$$

$$u \frac{\partial u}{\partial x} + v \frac{\partial u}{\partial y} = \frac{(\mu + k)}{\rho} \frac{\partial^2 u}{\partial y^2} + \frac{k}{\rho} \frac{\partial \omega}{\partial y} + g\beta(T - T_\infty)\cos\gamma + g\beta'(C - C_\infty)\cos\gamma - \frac{\sigma}{\rho} B_0^2(u - U_\infty) - \frac{v}{k_p} \frac{\partial \phi}{\partial y} (u - U_\infty) - \frac{c_b \phi}{\sqrt{k_p}} (u^2 - U_\infty^2) \quad (2.2)$$

$$u \frac{\partial \omega}{\partial x} + v \frac{\partial \omega}{\partial y} = \frac{\gamma^*}{\rho j} \frac{\partial^2 \omega}{\partial y^2} - \frac{k}{\rho j} \left(2\omega + \frac{\partial u}{\partial y} \right), \quad (2.3)$$

$$\rho c_p \left(u \frac{\partial T}{\partial x} + v \frac{\partial T}{\partial y} \right) = \kappa \frac{\partial^2 T}{\partial y^2} + Q(T - T_\infty) + (\mu + k) \left(\frac{\partial u}{\partial y} \right)^2 - \frac{\partial q_r}{\partial y}, \quad (2.4)$$

$$u \frac{\partial C}{\partial x} + v \frac{\partial C}{\partial y} = D^* \frac{\partial^2 C}{\partial y^2}. \quad (2.5)$$

Here v is kinematic viscosity, k represent vortex viscosity, g is acceleration by cause of gravity, thermal expansion factor is β , β' concentration expansion coefficient, μ is factor of viscosity, γ is angle of inclination, κ is thermal conductivity, ω is rotational velocity of particle, σ is fluid electrical conductivity, k_p is permeability coefficient of absorbent medium, ϕ represent porosity, C_b is drag coefficient which depend on geometry of the medium, at constant pressure specific heat is C_p , Q represent heat source/sink, radiative heat flux is q_r , U_∞ is free stream velocity, C is fluid concentration, C_∞ is free stream concentration, fluid temperature is T , T_∞ is free stream temperature, γ^* is spin gradient viscosity, density of micro inertia is j , D^* is molecular diffusivity.

Boundary conditions are:

$$u = L_1 \frac{\partial u}{\partial y}; v = -V_w; \omega = -m \frac{\partial u}{\partial y}; T = T_w + D_1 \frac{\partial T}{\partial y}; C = C_w \text{ at } y = 0. \quad (2.6)$$

$$u \rightarrow U_\infty; \omega \rightarrow 0; T \rightarrow T_\infty; C \rightarrow C_\infty; \text{ as } y \rightarrow \infty. \quad (2.7)$$

Here L_1 and D_1 are velocity and thermal slip factors given by $L_1 = L\sqrt{Re_x}$ and $D_1 = D\sqrt{Re_x}$, where L and D are initial values of velocity and thermal slip factor. $T_w = T_\infty + \frac{T_0}{x}$ is the variable temperature of the plate and V_w is the velocity of suction.

Here m is surface parameter lies between 0 and 1.

$\gamma = (\mu + \frac{\kappa}{2})j = \mu(1 + \frac{K}{2})j$, $j = \frac{vx}{U_\infty}$, $K = \frac{\kappa}{\mu}$ is the material parameter.

Using Roseland's approximation for radiation, we

obtain $q_r = -\left(\frac{4\sigma^*}{3k_1}\right)\frac{\partial T^4}{\partial y}$, where σ^* represents Stefan-Boltzmann constant, k_1 represents mean absorption factor. By using Taylor series about the free stream temperature, we have

$$T^4 = 4TT_\infty^3 - 3T_\infty^4. \quad (2.8)$$

Now eqn.(2.4) converts to

$$u \frac{\partial T}{\partial x} + v \frac{\partial T}{\partial y} = \frac{\kappa}{\rho c_p} \frac{\partial^2 T}{\partial y^2} + \frac{16\sigma^* T_\infty^3}{3k_1 \rho c_p} \frac{\partial^2 T}{\partial y^2} + \frac{Q(T - T_\infty)}{\rho c_p} + \left(\frac{\mu + k}{\rho c_p}\right) \left(\frac{\partial u}{\partial y}\right)^2. \quad (2.9)$$

3 Problem Solution

Introducing similarity transformation and dimensionless parameters

$$\Psi = (U_\infty x v)^{\frac{1}{2}} f(\eta), \eta = \left(\frac{U_\infty}{\nu x} \right)^{\frac{1}{2}} y,$$

$$\omega = U_\infty \left(\frac{U_\infty}{\nu x} \right)^{\frac{1}{2}} h(\eta), \quad (3.1)$$

$$\theta(\eta) = \frac{T - T_\infty}{T_w - T_\infty}, \quad \phi(\eta) = \frac{C - C_\infty}{C_w - C_\infty}.$$

Using equation (3.1) into equations (2.2), (2.3), (2.5) and (2.9) we get

$$(1 + K)f''' + \frac{1}{2}ff'' + Gr\theta\cos\alpha + Gc\phi\cos\alpha - Kh' + M(1 - f') - Da^{-1}(f' - 1) - \alpha(f'^2 - 1) = 0 \quad (3.2)$$

$$\left(1 + \frac{K}{2}\right)h'' + \frac{1}{2}fh' + \frac{1}{2}f'h - K(2h + f'') = 0, \quad (3.3)$$

$$\theta''(1 + R) + Pr.H.\theta + (1 + K)Ec.Pr f''^2 + \frac{1}{2}Pr f\theta' = 0, \quad (3.4)$$

$$\phi'' + \frac{1}{2}Sc.f.\phi' = 0. \quad (3.5)$$

The boundary conditions (2.6) and (2.7) are reduced

$$f' = S_v f'', f = S, h = -m f'', \theta = 1 + S_T \theta', \phi = 1 \text{ at } \eta = 0, \quad (3.6)$$

$$f' \rightarrow 1, \quad h \rightarrow 0, \quad \theta \rightarrow 0, \quad \phi \rightarrow 0 \text{ as } \eta \rightarrow \infty. \quad (3.7)$$

Where $Pr = \frac{\rho c_p \nu}{\kappa}$ signifies Prandtl number, $M = \frac{\sigma B_0^2}{\rho U_\infty}$ is magnetic parameter, $R = \frac{16\sigma^*}{3K_1\kappa} T_\infty^3$ is the radiation parameter, $Da^{-1} = \frac{\nu \varphi x}{k_p U_\infty}$ is inverse darcy number, $\alpha = \frac{c_b \varphi x}{\sqrt{k_p}}$ is local inertia coefficient parameter, $Sc = \frac{\nu}{D^*}$ is the Schmidt number, m is

surface condition parameter having range $0 \leq m \leq 1$, $K = \frac{\kappa}{\mu}$ is material parameter, H is heat source/sink parameter, Grashof number is Gr , Gc represent modified Grashof number, Ec appear for Eckert number, S is suction/injection parameter, S_v is velocity slip parameter and S_t is thermal slip parameter, which are defined as

$$H = \frac{Qx}{U_\infty \rho c_p}, \quad Gr = \frac{g\beta(T_w - T_\infty).x}{U_\infty^2}, \quad Gc = \frac{\beta'g(C_w - C_\infty)}{U_\infty^2}$$

$$Ec = \frac{u_\infty^2}{c_p(T_w - T_\infty)}, \quad S = 2\sqrt{\frac{x}{\nu U_\infty}} V_w, \quad S_v = L \frac{U_\infty}{\nu},$$

$$S_t = D \frac{U_\infty}{\nu} \quad (3.8)$$

The physical parameters of attention are skin friction factor C_f , local couple stress factor M_m , the Nusselt number Nu_x and Sherwood number Sh_x are given as follows

$$C_f = \frac{2\tau_w}{\rho U_\infty^2}, \quad (3.9)$$

$$M_m = \frac{c_m}{x\rho U_\infty^2}, \quad (3.10)$$

$$Nu_x = \frac{xq_w}{k(T_w - T_\infty)}, \quad (3.11)$$

$$Sh_x = \frac{xL_w}{D(C_w - C_\infty)}. \quad (3.12)$$

Here τ_w represents surface shear stress, c_m denote the couples stress, q_w is local surface heat flux and the local mass flux L_w are described as

$$\tau_w = [(\mu + k)\left(\frac{\partial u}{\partial y}\right) + k\omega]_{y=0}, \quad (3.13)$$

$$c_m = \gamma^*\left(\frac{\partial \omega}{\partial y}\right)_{y=0}, \quad (3.14)$$

$$q_w = -\kappa\left(\frac{\partial T}{\partial y}\right)_{y=0}, \quad (3.15)$$

$$L_w = -D^*\left(\frac{\partial C}{\partial y}\right)_{y=0}. \quad (3.16)$$

from equations (3.13) to (3.16) and

similarity transformations we get

$$Re_x^{\frac{1}{2}} C_f = 2[1 + (1 - m)K]f''(0), \quad (3.17)$$

$$Re_x M_m = \left(1 + \frac{K}{2}\right)h'(0), \quad (3.18)$$

$$Nu_x = -\theta'(0)Re_x^{\frac{1}{2}}, \quad (3.19)$$

$$Sh_x = -\phi'(0)Re_x^{\frac{1}{2}}. \quad (3.20)$$

Here $Re_x = U_\infty \frac{x}{\nu}$ represents local Reynolds number.

4 Numerical Solution

Eqn. (3.2) to (3.5) are solved numerically along

boundary conditions (3.6) and (3.7) by applying the shooting method together with RK4 scheme. For calculations we utilize MATLAB computer programming. Appropriate estimate values of $f''(0)$, $h'(0)$, $\theta'(0)$ and $\phi'(0)$ are taken with shooting technique to obtain boundary conditions at $\eta \rightarrow \infty$ which are one, zero, zero and zero respectively.

5 Discussion of the Results

For computation default values are $M = 1$, $Pr = 0.5$, $Ec = 0.5$, $m = 0.5$, $S = 2.15$, $K = 0.5$, $H = 0.1$, $Gr = 0.3$, $R = 0.5$, $Sc = 0.21$, $S_t = 0.3$, $S_v = 0.2$, $\gamma = \pi/3$, $Gc = 0$, $Da^{-1} = 0.2$, $\alpha = 0.2$.

From Fig.5.1, 5.2 and 5.3 it is observed that increase in the inverse Darcy number Da^{-1} , local inertia coefficient parameter α and Magnetic parameter M velocity profile increases, these results agree with [9]. Fig.5.4 depicts the effect of Grashof number on velocity profile, velocity increases with Gr increase on account of increase temperature gradient. From Fig.5.5 it is observed that velocity profile increase when modified Grashof number increase. Fig.5.6 represent velocity profiles increases for increasing values of radiation parameter R by reason that capacity of heat generation by thermal radiation increased, bond of fluid particles are quickly broken so, fluid velocity increase. Fig.5.7 describes that with increasing values of velocity slip parameter Fluid velocity enhances. From Fig.5.8 and 5.20 depicts increasing values of heat source parameter H enhance velocity and temperature profiles by reason of when heat is absorbed the buoyancy force account for enhances rate of flow and temperature. Velocity

decrease and microrotation profile increase with increasing Material parameter K as shown in Fig.5.9 and Fig.5.12. Fig.5.11 represent with increasing suction parameter S velocity increases due to making momentum boundary thinner. From Fig.5.10 it is observed that with more inclination of the plate velocity profile decrease. From Fig.5.11, Fig.5.14, Fig.5.15 and Fig.5.22 we conclude that velocity and microrotation profile increase with increasing values of suction S but opposite effects are found in temperature and concentration profile. Fig. 5.13 illustrates that with increasing values of velocity slip parameter S_v , microrotation profile increase. From Fig. 5.16 observed that thermal boundary layer reduces with increasing values of thermal slip parameter. Fig.5.17 represent temperature profile with variation in Prandtl number Pr . This figure shows that increase in values of Pr temperature decreases due to the fact that Prandtl number is proportional to the specific heat i.e. more the heat require to increase the temperature for a unit mass of a given substance by a given amount. Fig.5.18 shows that when we increase Eckert number then temperature profile increases because when we increase the Ec then viscous dissipation increase due to this self heating in fluid increase, so temperature increase. Fig.5.19 represents temperature profiles increase with Radiation parameter in view of increment in value of R reduce Roseland radiation absorptivity K_1 , the radiative heat flux increases as K_1 decreases i.e. radiative heat transfer rate to fluid will increase so, fluid temperature increases. Thickness of thermal boundary layer decreases with increasing thermal slip temperature parameter S_t so temperature decrease. Fig. 5.21 shows the effect of Schmidt number Sc on concentration profile. Increase in Schmidt number reduce concentration profile by reason of molecular diffusivity reduce with increment in Schmidt number.

Table 5.1 represents the behavior of $f''(0)$, $h'(0)$, $\theta'(0)$ and $\phi'(0)$ for various values of flow parameters. From table we observed that $f''(0)$, $h'(0)$, $\phi'(0)$ have increasing behavior for increasing values of Da^{-1} , α , M , Gr , Ec but diminishing behavior for $\theta'(0)$. For Pr and γ opposite results are found.

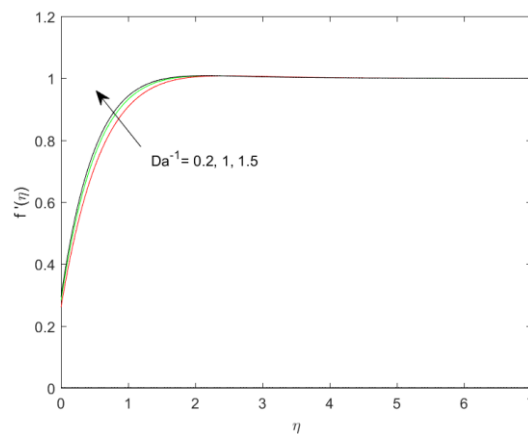


Fig. 5.1: Distribution of velocity for variations in Da^{-1}

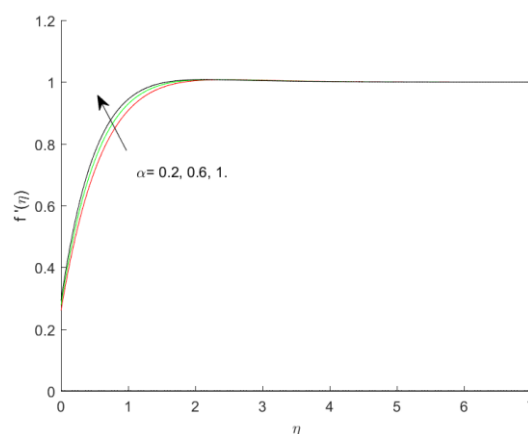


Fig. 5.2: Distribution of velocity for variations in $alpha$

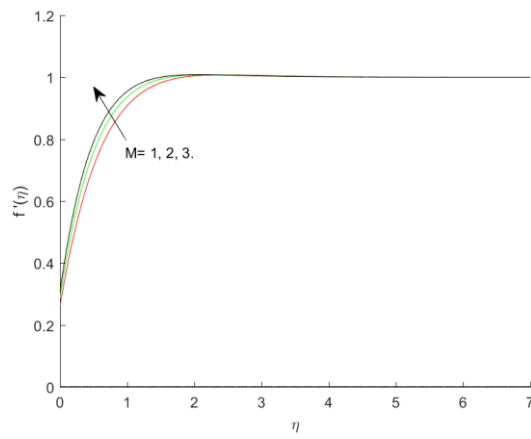


Fig. 5.3: Distribution of velocity for variations in M

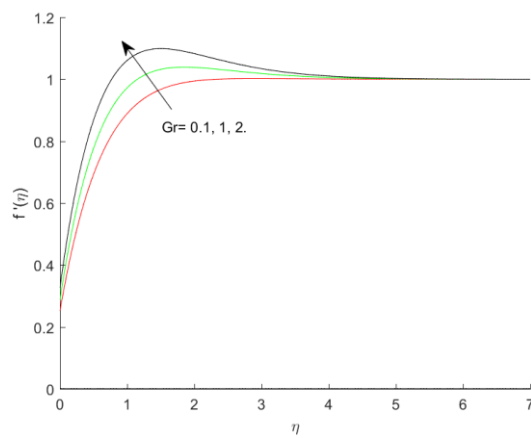


Fig. 5.4: Distribution of velocity for variations in Gr

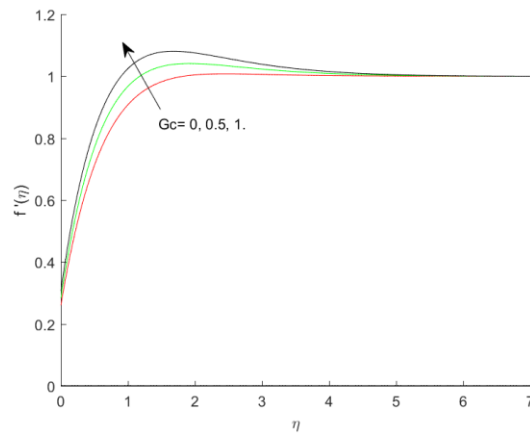


Fig. 5.5: Distribution of velocity for variations in Gc

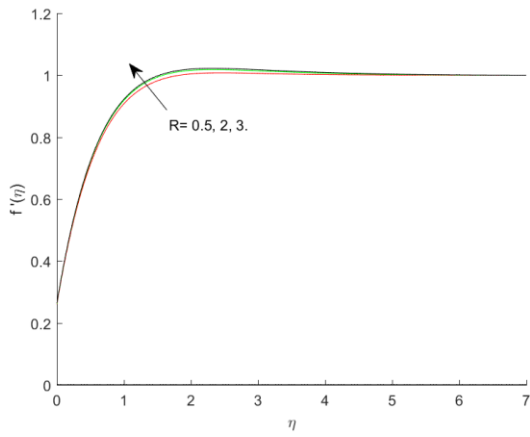


Fig. 5.6: Distribution of velocity for variations in R

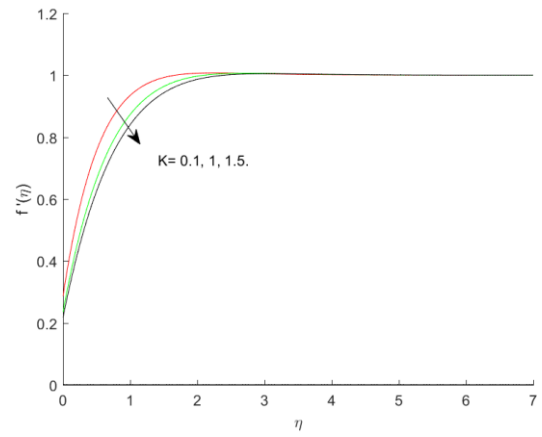


Fig. 5.9: Distribution of velocity for variations in K

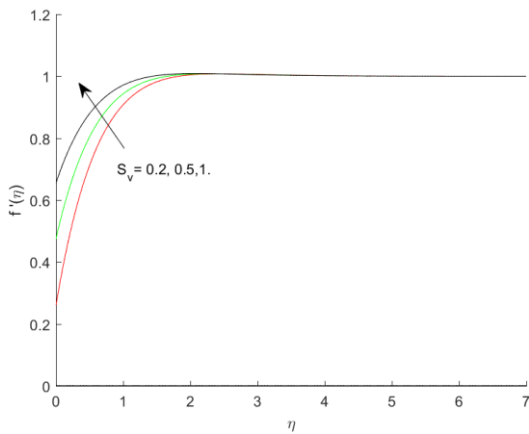


Fig. 5.7: Distribution of velocity for variations in S_v

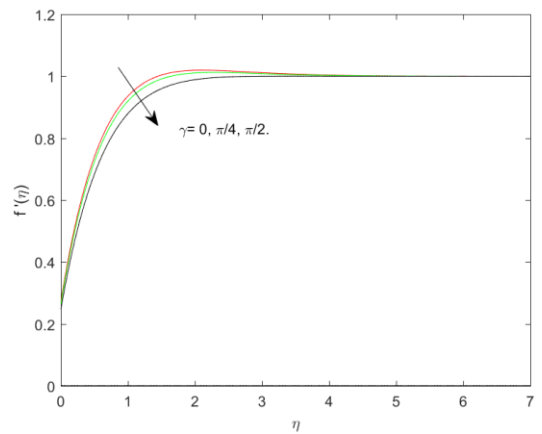


Fig. 5.10: Distribution of velocity for variations in γ

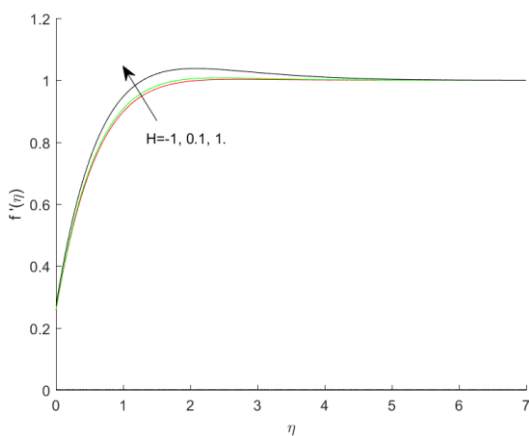


Fig. 5.8: Distribution of velocity for variations in H

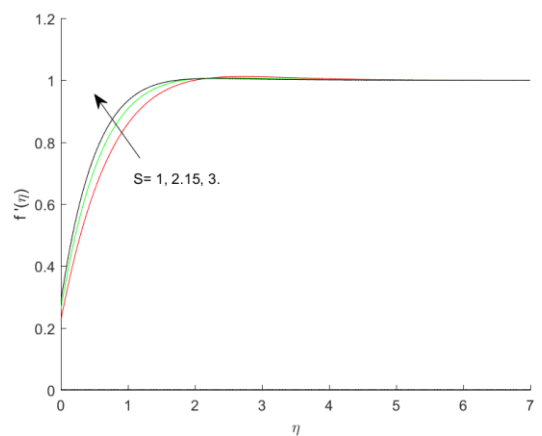


Fig. 5.11: Distribution of velocity for variations in S

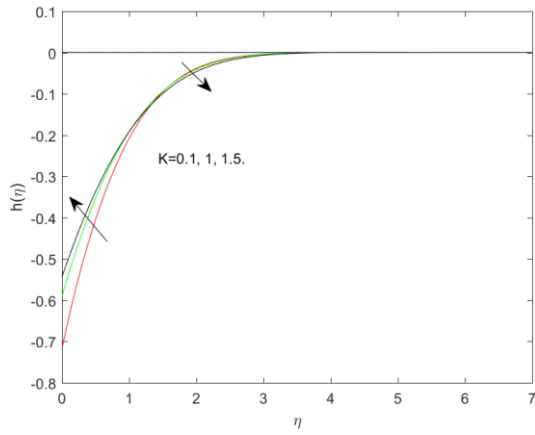


Fig. 5.12: Distribution of microrotation for variations in K

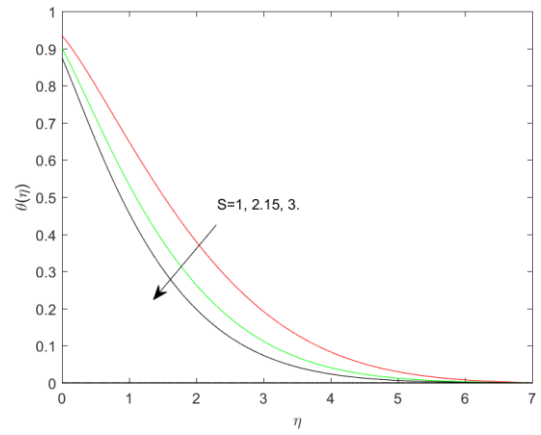


Fig. 5.15: Distribution of temperature for variations in S

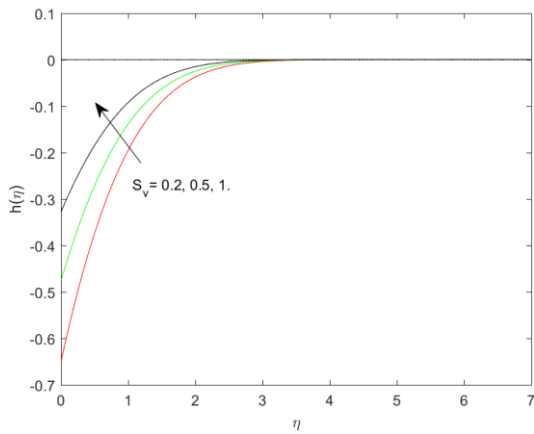


Fig. 5.13: Distribution of microrotation for variations in S_v

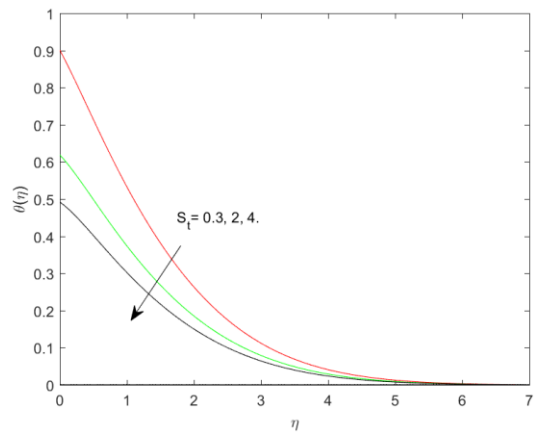


Fig. 5.16: Distribution of temperature for variations in S_t

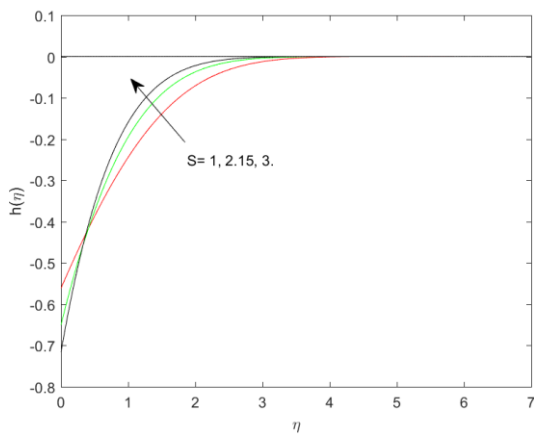


Fig. 5.14: Distribution of microrotation for variations in S

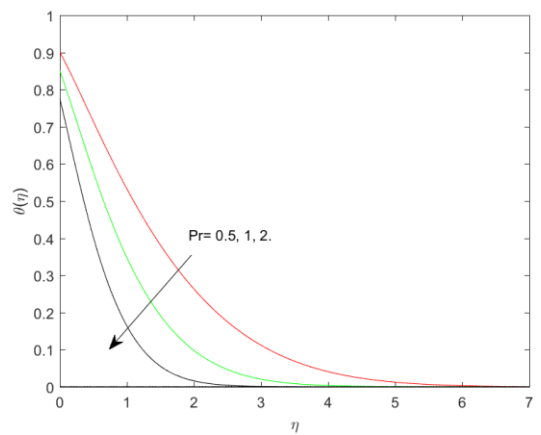


Fig. 5.17: Distribution of temperature for variations in Pr

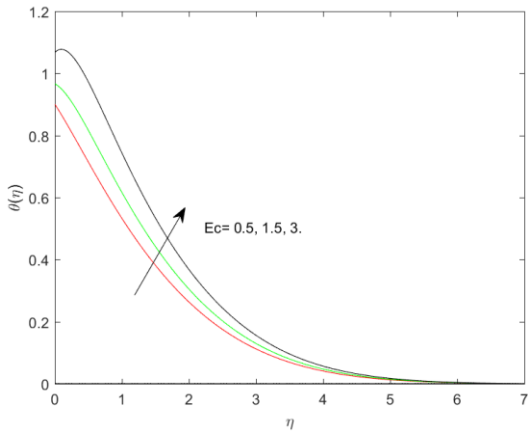


Fig. 5.18: Distribution of temperature for variations in Ec

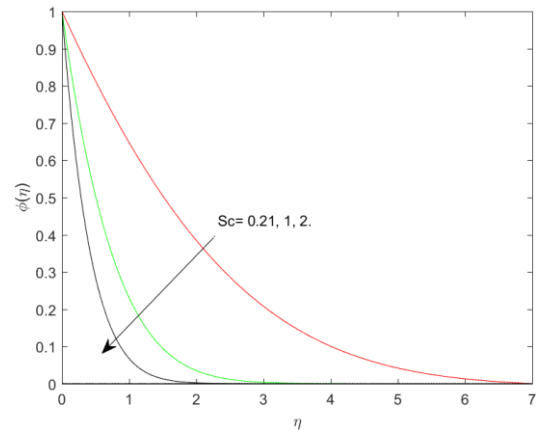


Fig. 5.21: Distribution of concentration for variations in Sc

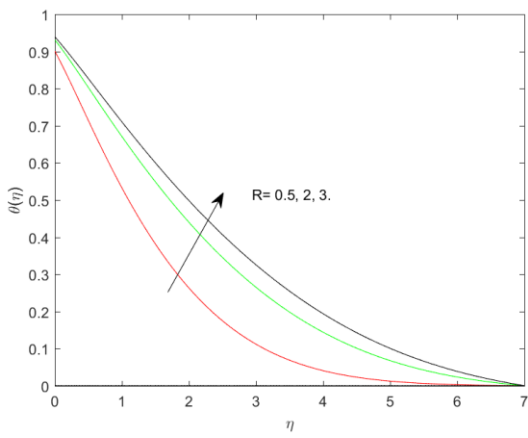


Fig. 5.19: Distribution of temperature for variations in R

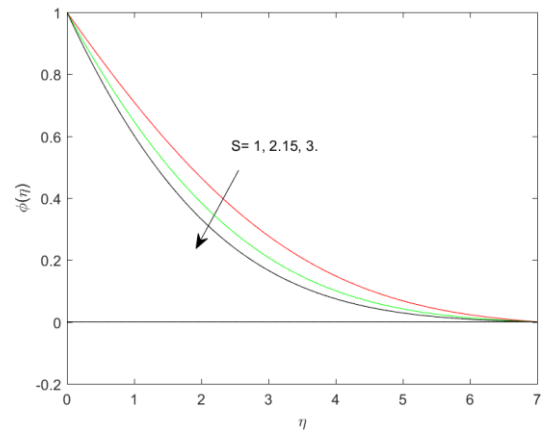


Fig. 5.22: Distribution of concentration for variations in S

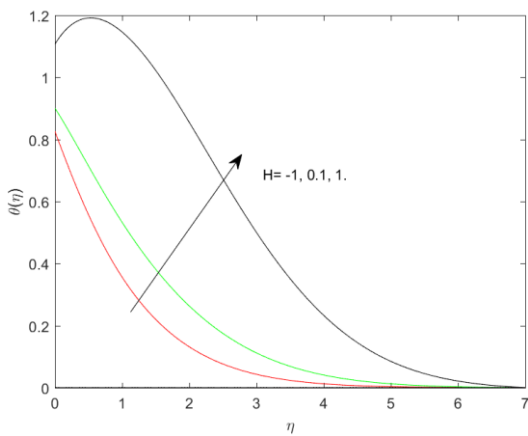


Fig. 5.20: Distribution of temperature for variations in H

Table 5.1: For variations in values of Da^{-1} , α , M , Gr , Pr , S , Ec , R , Sc and γ , Values of $f''(0)$, $h'(0)$, $-\theta'(0)$ and $-\phi'(0)$.

Da^{-1}	α	M	Gr	Pr	S	Ec	R	Sc	γ	$f''(0)$	$h'(0)$	$-\theta'(0)$	$-\phi'(0)$
0.2										1.30047	0.66761	0.33260	0.39760
1										1.41080	0.74549	0.33100	0.40000
1.5										1.46951	0.78715	0.32940	0.40120
	0.2									1.30047	0.66761	0.33260	0.39760
	0.6									1.38833	0.72953	0.33030	0.39960
	1									1.46395	0.78337	0.32847	0.40120
		1								1.30047	0.66761	0.33260	0.39760
		2								1.43517	0.76305	0.32980	0.40050
		3								1.54215	0.83921	0.32840	0.40250
			0.1							1.26047	0.64142	0.33500	0.39590
			1							1.43890	0.75842	0.32350	0.40310
			2							1.63370	0.88660	0.30770	0.41060
				0.5						1.30047	0.66761	0.33260	0.39760
				1						1.28232	0.65851	0.50080	0.39670
				2						1.27100	0.64961	0.75050	0.39600
					1					1.12230	0.37552	0.21830	0.30820
					2.15					1.30047	0.66761	0.33260	0.39760
					3					1.43227	0.9445	0.41830	0.46840
						0.5				1.30047	0.66761	0.33260	0.39760
						1.5				1.30853	0.67280	0.11260	0.39790
						3				1.32083	0.68080	-0.22500	0.39850
							0.5			1.30047	0.66761	0.33260	0.39760
							2			1.31402	0.67514	0.23010	0.39860
							3			1.31831	0.67721	0.20350	0.39900
								0.21		1.30047	0.66761	0.33260	0.39760
								1		1.30047	0.66761	0.33260	1.29460
								2		1.30047	0.66761	0.33260	2.3652
									0	1.36003	0.70660	0.32900	0.40000
									$\pi/4$	1.32520	0.68385	0.33120	0.39860
									$\pi/2$	1.24041	0.6284	0.33600	0.39520

6 Conclusions

In this paper a theoretical analysis of impact of thermal radiation and viscous dissipation on heat and mass transfer in *MHD* non-darcian flow of micropolar fluid along an inclined porous plate embedded in porous media. We have acquired following results:

- (i) An increase in inverse Darcy number, local inertia coefficient and magnetic parameter causes increment in skin friction coefficient.
- (ii) Velocity profile decrease with more inclination of the plate and the material parameter.
- (iii) Microrotation profile increase with increasing material parameter K , suction and decrease with surface parameter.

(iv) Temperature profile increase with increasing values of Eckert number, Radiation parameter, Heat source parameter and decrease with Prandtl number.

(v) Concentration profile decrease for increasing Schmidt number and suction parameter.

7 References

- [1] E. O. Fatunmbi and A. Adeniyani, “MHD stagnation point-flow of micropolar fluids past a permeable stretching plate in porous media with thermal radiation, chemical reaction and viscous dissipation”, *Journal of Advances in Mathematics and Computer Science*, vol. 26(1), pp. 1-19, Jan. 2018.
- [2] A.C. Eringen, “Theory of micropolar fluids”, *Journal of Mathematics and Mechanics*, vol. 16, pp. 1-18, July 1966.
- [3] A.C. Eringen, “Theory of Thermo micro fluids”, *Journal of Mathematical Analysis and Applications*, vol. 38, pp. 480-496, May 1972.
- [4] P. R. Sharma and Sharad Sinha, “MHD mixed convective slip flow, heat and mass transfer along a vertical porous plate”, *Journal of International Academy of Physical Sciences*, vol. 19(4), pp. 295-311, Sept. 2015.
- [5] Dulal Pal and Sewli Chatterjee, “Heat and mass transfer in MHD non-Darcian flow of a micropolar fluid over a stretching sheet embedded in a porous media with non-uniform heat source and thermal radiation”, *Commun Nonlinear Sci Numer Simulat*, vol. 15, pp. 1843-1857, July 2009.
- [6] Muhammad Ijaz Khan, Muhammad Waqas, Tasawar Hayat and Ahmed Alsaedi, “Chemically reactive flow of micropolar fluid accounting viscous dissipation and Joule heating”, *Results in Physics*, vol. 7, pp. 3706–3715, Sept. 2017.
- [7] R.S. Tripathy, G.C. Dash, S.R. Mishra, Mohammad Mainul Hoque, “Numerical analysis of hydromagnetic micropolar fluid along a stretching sheet embedded in porous medium with non-uniform heat source and chemical reaction”, *Engineering Science and Technology, an International Journal*, vol. 19, pp. 1573–1581, May 2016.
- [8] Ali J. Chamkha, S.M.M. EL-Kabeir and A.M. Rashad, “Coupled heat and mass transfer by MHD natural convection of micropolar fluid about a truncated cone in the presence of radiation and chemical reaction”, *Journal of Naval Architecture and Marine Engineering*, vol. 10, pp. 139-150, Dec. 2013.
- [9] S. N. Sahoo, “Heat and mass transfer effect on MHD flow of a viscoelastic fluid through a porous medium bounded by an oscillating porous plate in slip flow regime”, *Hindawi Publishing Corporation International Journal of Chemical Engineering*, vol. 2013, pp. 1-10, June 2013.